



Since 1969

DOI: <https://doi.org/10.54693/piche.05324>

Synthesis, Spectral Characterization, and Antimicrobial Evaluation of a Zn/Ni Bimetallic Complex Derived from 2,2'-Bipyridine-4,4'-Dicarboxylic Acid

F. Keerio¹, A. Shah^{1*}, M.Y. Talpur¹

Submitted: 29/11/2025, Accepted: 20/01/2026, Published: 04/02/2026

Abstract

Bimetallic complexes have garnered significant attention in the scientific community due to their versatile applications, such as antibacterial, antifungal, antitubercular, antimalarial, antioxidant, antibiotic, anti-inflammatory, and anticancer activities. This study reports the synthesis and characterization of a bimetallic Zn/Ni complex derived from 2,2'-bipyridine-4,4'-dicarboxylic acid (BPyCOOH) as a multifunctional coordination compound with effective antimicrobial impact. This complex ensured efficient coordination of the ligand with both Zn(II) and Ni(II) ions due to its bifunctional groups in a single ligand structure. Structural elucidation was achieved through UV-Vis, FTIR, and elemental analyses. The UV-Vis spectrum displayed two distinct absorption bands at approximately 280 nm and 400 nm, attributed to $\pi-\pi^*$ transitions and metal-to-ligand charge transfer (MLCT), confirming the successful formation of the bimetallic coordination framework. The Zn/Ni(BPyCOOH)₂ complex was evaluated for its antimicrobial potential against selected Gram-positive and Gram-negative bacterial strains, also demonstrating minimum inhibitory concentration (MIC) activity. The Gram-positive bacteria, *P. mirabilis*, showed the highest zones of inhibition (27.7±0.9) at (20 mg/ml) of Zn/Ni(BPyCOOH)₂ complex. Therefore, Zn/Ni(BPyCOOH)₂ complex shows concentration (dose) dependent antimicrobial activity. It is most effective against *Proteus mirabilis* (*P. mirabilis*), gram-negative, and least in *Staphylococcus aureus* (*S. aureus*), gram-positive, by calculating the diameter of the zone of inhibition. No inhibition observed in the control, which proves the results are valid.

Keywords: Ni and Zn Complex; Bimetallic Complex; Synthesis; UV-Vis; FTIR; SEM; XRD; Antimicrobial Activities.

1. Introduction:

Bioactive metal complexes containing bipyridine and other nitrogen donor ligands (such as phenanthroline, Schiff bases, etc.) have gained significant importance in coordination chemistry due to their rich structural diversity and multifunctional properties [1-5].

2,2'-Bipyridine 4,4'-dicarboxylic acid is a widely used ligand due to its dual functionality as a strong chelating agent and a versatile building block, specifically as an anchoring group in material science and metal-organic frameworks (MOFs). This combination of diverse applications features makes this ligand highly useful in a wide range of fields, like catalysis (e.g., for CO₂,

cycloaddition reactions), materials Science (MOFs) for gas storage, separation, and wastewater treatment), optoelectronics (dye-sensitized solar cells and LEDs), and medicine (metal complexes exhibiting anticancer and antibacterial properties) [6-8].

The design and synthesis of bimetallic coordination complexes have attracted considerable attention owing to their enhanced physicochemical, catalytic, and biological properties compared to their monometallic counterparts [9, 10]. Amongst several ligands, 2,2'-bipyridine-4,4'-dicarboxylic acid (BPyCOOH) is particularly noteworthy ligand because of its strong chelating ability and versatile coordination behavior

¹ Dr. M.A. Kazi, Institute of Chemistry, University of Sindh, Jamshoro, Sindh, Pakistan.

* Corresponding author: Ambreen Shah (ambreen.shah@usindh.edu.pk)

through nitrogen and oxygen donor sites [11, 12]. The incorporation of two different metal centers, such as Zn(II) and Ni(II), within a single complex can produce potential effects that enhance electron transfer, stability, and biological functionality [13, 14].

The primary advantage of a bimetallic zinc (Zn) and nickel (Ni) complex of 2,2'-bipyridine-4,4'-dicarboxylic acid is the powerful combination of the unique chemical properties of both metals, potentially leading to enhanced or novel functions not seen in their monometallic counterparts [15, 16].

Bimetallic complexes often exhibit superior biological activities (e.g., antibacterial, antifungal, or anticancer) compared to their monometallic analogues. The combination of Zn (an essential trace element with its own biological roles) and Ni (which has known antimicrobial and antioxidant activities) can result in a more potent agent, potentially through different mechanisms of action or improved cell permeability [17, 18]. The tailored bimetallic Zn/Ni(BPyCOOH)₂ complex therefore represents a promising candidate for exploring structure–activity relationships in multifunctional coordination systems [19].

Several studies have reported the synthesis and biological evaluation of metal complexes derived from substituted bipyridine ligands, highlighting their promising physicochemical and biological characteristics [20, 21]. Bipyridine-based ligands, owing to their π -conjugated framework and nitrogen donor sites, readily form stable chelates with transition metals such as Ni(II), Zn(II), Cu(II), and Co(II), thereby enhancing their redox activity and coordination geometry flexibility [22, 23]. Previous studies have demonstrated that Ni(II) complexes of bipyridine derivatives exhibit significant antimicrobial and antioxidant activities, attributed to their ability to interact with microbial cell membranes and disrupt metabolic pathways [24, 25]. Similarly, Zn(II) complexes are reported to possess broad-spectrum antibacterial and antifungal properties, often linked to their capacity to generate reactive oxygen species and inhibit enzyme function [26, 27]. Recent advances in bimetallic complex chemistry suggest that incorporating two metal ions within a single molecular framework can yield enhanced electron transfer, thermal stability, and bioactivity [28-30].

These studies involve bipyridine-4,4'-dicarboxylic acid as a bridging ligand and has revealed that the presence of carboxylate groups not only increases solubility and coordination versatility but also facilitates metal–ligand charge-transfer transitions, which influence biological performance. Initially, the Ni(BPyCOOH)₂ complex was obtained from the reagent 2,2'-bipyridine-4,4'-dicarboxylic acid; a bimetallic Zn/Ni(BPyCOOH)₂ complex was formed, which represents a logical extension of this research direction, aiming to explore the interplay between structure, electronic transitions, spectral characterization, and antimicrobial efficacy against selected bacterial strains.

2. Experimental Work:

2.1. Chemicals and Reagents:

Analytical reagent grade chemicals 2, 2'-bipyridine 4,4'-dicarboxylic acid (BPyCOOH), nickel (II) acetate (Ni(CH₃COO)₂ · 4H₂O), zinc (II) acetate (Zn(CH₃COO)₂), methanol (CH₃OH), pyridine (C₅H₅N), dimethyl sulfoxide (DMSO), and n-hexane were bought from E. Merck, Germany.

2.2. Instrumentation:

Elemental microanalysis was conducted by an instrument (Elemental Micro-Analysis Ltd, U.K). The FT-IR spectra were obtained on a new Infrared instrument (Nicolet Avatar 330 FT-IR (Thermo Nicolet Electron Corporation, USA), having a range between 4000-600 cm⁻¹. UV-Vis Spectrophotometer (a double beam Hitachi 220 spectrophotometer (Tokyo, Japan), with dual 1 cm silica cuvettes within 185-700 nm). Scanning Electron Microscopy with Energy Dispersive analysis (SEM-EDX) instrument, and X-Ray analysis was conducted on a diffraction (XRD) analysis, Phenom-World instrument.

2.3. Synthesis of Nickel Complex of [2,2'-Bipyridine-4,4'-Dicarboxylic Acid] Ni(BPyCOOH)₂:

The synthesis of the nickel metal complex Ni(BPyCOOH)₂ is a general method for complexation [33]. The procedure is given below:

0.2 M solution of 2,2'-bipyridine-4,4'-dicarboxylic acid was prepared in 15 mL of a 1:1 (v/v) mixture of methanol (CH₃OH) and DMSO. Separately, a 0.1 M solution of Ni (II) acetate was prepared in 10 mL of methanol to make a (1:2) metal complex solution. The Ni (II) acetate solution was added dropwise to the ligand solution under continuous stirring. The reaction mixture was then refluxed for 2 hrs at 85 °C. Upon completion, the mixture

was poured into chilled distilled water to precipitate the complex. The resulting solid was filtered, washed thoroughly with distilled water, dried, and recrystallized from a methanol/n-hexane solvent system to afford the Ni(BPyCOOH)₂ complex.

2.4. Synthesis of Bimetallic Complex of 2,2'-Bipyridine-4,4'-Dicarboxylic Acid Zn/Ni (BPyCOOH)₂:

The synthesis bimetal complex Zn/Ni(BPyCOOH)₂ is a modified form [15], and the procedure is given below:

A 1 M solution of the pre-synthesized nickel complex, Ni(BPyCOOH)₂, was prepared in methanol. To this solution, a 2 M zinc acetate solution (prepared in 10 mL of methanol) was added slowly under constant stirring. The resulting mixture was refluxed for 1.5 hrs at 85 °C to ensure complete complexation. After refluxing, the mixture was poured into chilled distilled water to induce precipitation of the bimetallic complex. The obtained solid was filtered, washed, dried, and recrystallized from a methanol/n-hexane solvent system to yield the Zn/Ni(BPyCOOH)₂ complex.

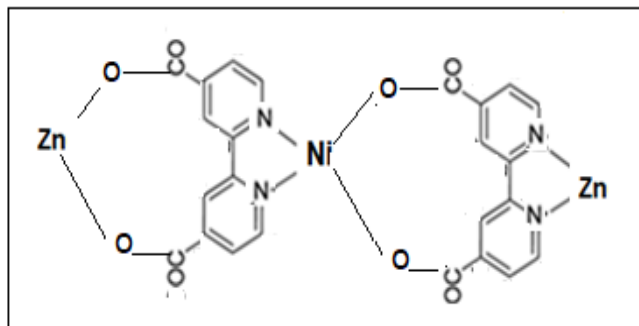


Figure 1: The structural diagram of a bimetallic Zn/Ni(BPyCOOH)₂ complex

2.5. Antimicrobial Study of Bimetallic (II) complex Zn/Ni(BPyCOOH)₂:

The bimetallic metal (II) complex Zn/Ni(BPyCOOH)₂ was screened for *in vitro* antibacterial activity against several bacterial strains, including *Bacillus licheniformis* (*B. licheniformis*), *Proteus mirabilis* (*P. mirabilis*), *Staphylococcus aureus* (*S. aureus*), and *Escherichia coli* (*E. Coli*).

2.5.1. Determination of the Diameters of the Zone of Inhibition:

The diameters of the zone of inhibition of the synthesized Zn/Ni(BPyCOOH)₂ complex were determined using the agar well diffusion method [10]. All

equipment used for the incubation test was washed properly and rinsed with 96% ethyl alcohol. The stock solution (1 mg/mL) of the metal complex compound was prepared in DMSO. For determining the zone of inhibition, the medium was poured into a Petri dish and allowed to solidify at room temperature. Wells were made on the solidified medium, and the prepared solutions were added to the wells and allowed to diffuse. The indicator organisms were overlaid onto the agar medium, and the plates were incubated at 37°C for 24 hours for the bacteria. The antimicrobial activities were assessed by measuring the diameter of the zone of inhibition of bacterial growth around each well along two axes. For each product tested, three determinations were made.

2.5.2. Minimum Inhibitory Concentration:

The minimum inhibitory concentrations (MICs) were determined by the microdilution method in a 96-well microplate for the bacterial species [31]. The quantitative solutions of 5, 10, and 20 mg/1ml Zn/Ni(BPyCOOH)₂ complex were determined against four bacterial strains, including Gram-positive (*S. aureus* and *B. licheniformis*) and Gram-negative bacteria (*E. coli*, and *P. mirabilis*) by calculating the diameter of the zone of inhibition.

3. Results and Discussions:

3.1. Characterization Study:

The proposed molecular structure of the heterometallic coordination complex comprises Ni(II) and Zn(II) metal centers bridged through 2,2'-bipyridine-4,4'-dicarboxylate ligands shown in Fig. 1. In this structure, the central Ni(II) ions exhibits an octahedral geometry, being coordinated by two bidentate bipyridine ligands through their nitrogen donor atoms and by two oxygen atoms, possibly originating from acetate or solvent molecules, thereby completing the six-coordinate environment. Each Zn(II) ion adopts a tetrahedral geometry, coordinated to two oxygen atoms from the carboxylate groups of the bipyridine ligands and two additional oxygen atoms from acetate groups. The carboxylate moieties act as bridging linkers, facilitating metal-to-metal connectivity between the Ni and Zn centers. This arrangement results in a supramolecular heteronuclear assembly that enhances electronic communication, structural stability, and functional properties of the complex, making it potentially useful for applications in biological systems, catalysis, sensing, and photochemical processes [16, 17].

3.2. FTIR Spectroscopy:

FT-IR spectra of the $\text{Ni}(\text{BPyCOOH})_2$ complex and its mixtures with various concentrations of zinc acetate (0.05 M, 0.1 M, and 0.25 M) were recorded to analyze changes in vibrational characteristics. FTIR spectroscopy was employed to identify functional groups and examine metal–ligand interactions based on characteristic vibrational frequencies. The broad band around 3400 cm^{-1} corresponds to the $-\text{OH}$ stretching vibration, which becomes less intense and slightly shifts with increasing Zn concentration, indicating hydrogen bonding and possible coordination changes involving hydroxyl groups. The peak near 1650 cm^{-1} represents the $\text{C}=\text{O}$ stretching vibration, showing reduced intensity in Zn-containing samples, suggesting partial coordination of Zn(II) ions with the carboxylate oxygen atoms of $\text{Zn}/\text{Ni}(\text{BPyCOOH})_2$. The band in the 1380 cm^{-1} region corresponds to $\text{O}-\text{C}-\text{O}$ stretching, confirming the presence of carboxylate ligands, Fig. 2. In the lower region, a peak appeared at 480 cm^{-1} due to metal–oxygen interactions ($\text{Ni}-\text{O}$ band), while this peak shifts to a higher region with increasing molar concentrations of Zn metal.

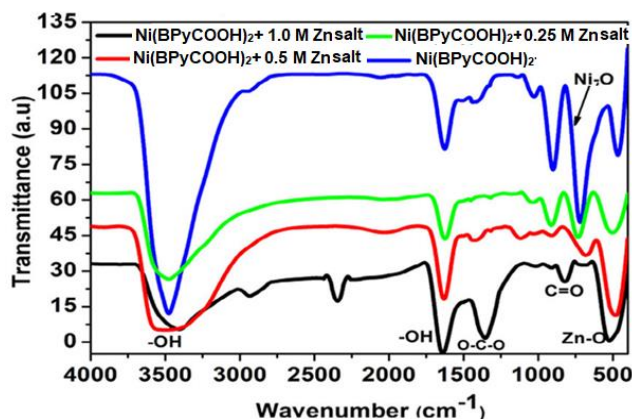


Figure 2: FTIR spectra of $\text{Ni}(\text{BPyCOOH})_2$, and the bimetallic $\text{Zn}/\text{Ni}(\text{BPyCOOH})_2$ complex of 2,2'-bipyridine-4,4'-dicarboxylic acids at different concentrations.

3.3. UV-Visible Spectroscopy:

The UV–Vis spectrum of the bimetallic $\text{Zn}/\text{Ni}(\text{BPyCOOH})_2$ complex displayed two prominent absorption peaks, indicating the presence of multiple electronic transitions within the molecule, Fig. 3. The first strong absorption band appeared at 280 nm , corresponding to $\pi \rightarrow \pi^*$ transitions of the aromatic bipyridine ligand, confirming successful coordination between the ligand and the metal centers [21–22]. A second, less intense band observed at 412 nm was attributed to metal-to-

ligand charge transfer (MLCT), signifying interactions between the Ni(II) and Zn(II) ions and the conjugated system of the ligand. The gradual decrease in absorbance beyond 500 nm reflects the limited $d-d$ transitions typical for low-spin d^8 and d^{10} metal centers in octahedral or distorted octahedral geometries [28].

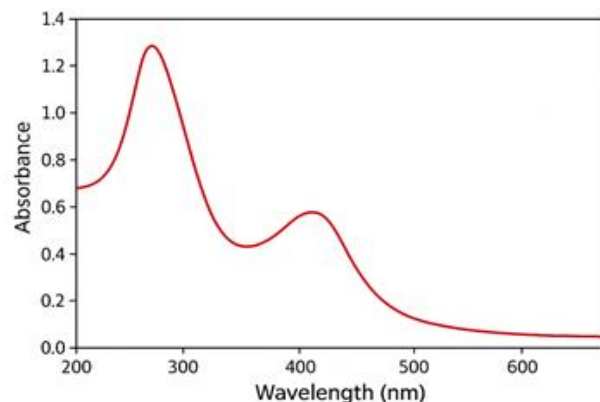


Figure 3: UV–Vis spectrum of the bimetallic complex of 2,2'-bipyridine-4,4'-dicarboxylic acids $\text{Zn}/\text{Ni}(\text{BPyCOOH})_2$

3.4. SEM Spectroscopy:

The SEM (Scanning Electron Microscopy) images of a series of bimetallic $\text{Zn}/\text{Ni}(\text{BPyCOOH})_2$ complexes synthesized from $\text{Ni}(\text{BPyCOOH})_2$ in the presence of varying concentrations of zinc salt. The micrographs were magnified $5000\times$ with a scale bar of $5\text{ }\mu\text{m}$, illustrating the morphological evolution of the $\text{Ni}(\text{BPyCOOH})_2$ complex as Zn(II) ions were introduced in increasing molar concentrations.

The SEM images of the bimetallic Zn/Ni complexes were obtained under different magnetic field intensities. At low Zn(II) concentrations, small spherical particles began to appear, but they were slightly aggregated compared to the pure $\text{Ni}(\text{BPyCOOH})_2$ complex. This suggests that Zn(II) ions acts as nucleation centers, slightly modifying the growth pattern of the $\text{Ni}(\text{BPyCOOH})_2$ complex.

As the concentration of Zn (II) ions increased, the surface morphology became denser and more compact, as shown in Fig. 4. Larger and more agglomerated particles were observed, indicating enhanced crystal growth due to the higher availability of Zn(II) ions, which likely facilitated particle fusion. At the highest Zn(II) concentration, the morphology exhibited distinct spherical agglomerates with increased particle size. Therefore, the increasing Zn salt concentration significantly influenced the surface morphology, particle

size, and aggregation behavior of the $\text{Ni}(\text{BPyCOOH})_2$ complex. This morphological tuning could have affected the catalytic, optical, or adsorption properties of the resulting material, making the $\text{Zn}/\text{Ni}(\text{BPyCOOH})_2$ system potentially more effective for applications such as biological activities, pollutant removal, catalysis, or electrochemical sensing.

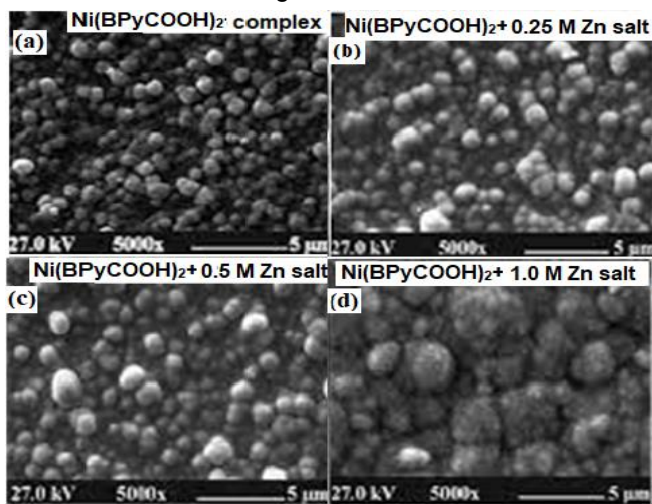


Figure 4: SEM images of $\text{Ni}(\text{BPyCOOH})_2$, and the bimetallic $\text{Zn}/\text{Ni}(\text{BPyCOOH})_2$ complex of 2,2'-bipyridine-4,4'-dicarboxylic acids at different concentrations of $\text{Zn}(\text{II})$ salt

3.5. EDS Spectroscopy:

The Energy Dispersive X-ray Spectroscopy (EDX) spectrum of the synthesized $\text{Ni}(\text{BPyCOOH})_2$ complex modified with Zn salt, provided qualitative and semi-quantitative information about the elemental composition of the sample. The prominent peaks observed in the spectrum corresponded to the elements C (carbon), O (oxygen), Ni (nickel), Zn (zinc), and Al (aluminum).

The intense peaks of O (oxygen) around 0.52 keV and C near 0.28 keV confirmed the presence of oxygen and carbon-containing functional groups originating from the bipyridine ligand and possibly from residual organic precursors, can be seen in Fig. 5. The distinct peaks of Ni (~0.85 keV) and Zn (~1.0 keV) verified the successful incorporation of both metallic species into the Ni–Zn–bipyridine framework.

Thus, the EDX spectrum confirmed that the composite material primarily consisted of Ni, Zn, O, and C elements, validating the successful synthesis of the Ni–Zn bipyridine complex. The relative intensities of the peaks indicated a homogeneous distribution of these elements, suggesting that Zn ions were well integrated

within the Ni complex matrix, thereby enhancing the structural stability and functional performance of the material.

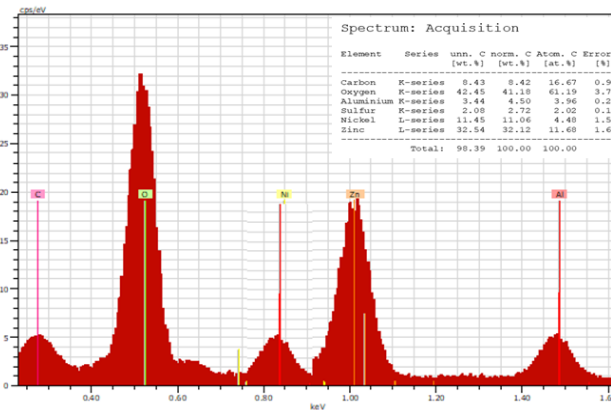


Figure 5: EDS images of the bimetallic $\text{Zn}/\text{Ni}(\text{BPyCOOH})_2$ complex of 2,2'-bipyridine-4,4'-dicarboxylic acids

3.6. X-ray Diffraction:

This figure represented the X-ray diffraction (XRD) patterns of $\text{Zn}/\text{Ni}(\text{BPyCOOH})_2$ complexes synthesized in the presence of different concentrations of Zn salt (0.25 M, 0.5 M, and 1.0 M) in the $\text{Ni}(\text{BPyCOOH})_2$ metal complex, as shown in Fig. 6. The sample of $\text{Ni}(\text{BPyCOOH})_2$ with 0.25 M Zn salt showed prominent peaks corresponding to ZnO, with major diffraction planes indexed at (100), (101), and (102), confirming the formation of a wurtzite hexagonal ZnO phase. These peaks indicated that at lower Zn concentrations, ZnO was the dominant crystalline phase formed along with the Ni–bipyridine matrix.

For the $\text{Ni}(\text{BPyCOOH})_2$ sample containing 0.5 M Zn salt, the diffraction peaks appeared sharper and more intense, showing well-defined reflections corresponding to the ZnO (100, 002, 101, and 102) planes, which suggested enhanced crystallinity. In the case of $\text{Ni}(\text{BPyCOOH})_2$ with 1.0 M Zn salt, the XRD pattern exhibited characteristic peaks for metallic Zn (100, 101, 103). The ZnO peaks disappeared, while the Ni–Zn alloy peaks indicated a phase transition from an oxide-dominated structure to an intermetallic phase at higher Zn concentrations. The increased Zn content likely promoted reduction and alloy formation, resulting in a more metallic character of the synthesized material [30].

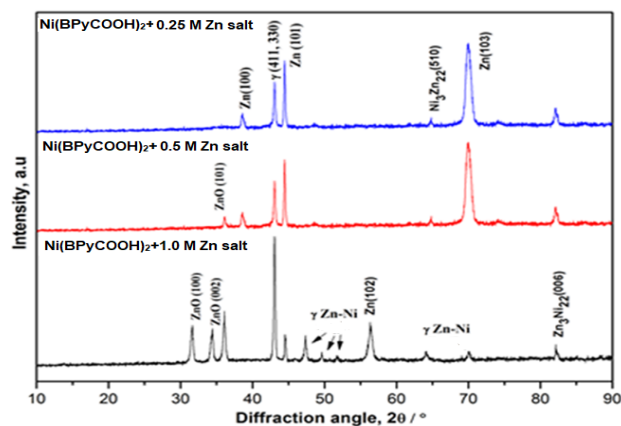


Figure 6: XRD spectra of the bimetallic Zn/Ni(BPyCOOH)₂ complex of 2,2'-bipyridine-4,4'-dicarboxylic acids at different concentrations of Zn(II) salt

3.7. Antimicrobial Activity of Bimetallic Complexes Zn/Ni(BPyCOOH)₂:

3.7.1. Determination of the Diameters of the Zone of Inhibition (DZI):

The diameters of the zone of inhibition of the Zn/Ni(BPyCOOH)₂ complex were successively obtained using the agar well diffusion method [31-32]. The diameters of the zone of inhibition of the bacteria are summarized in Fig. 7.

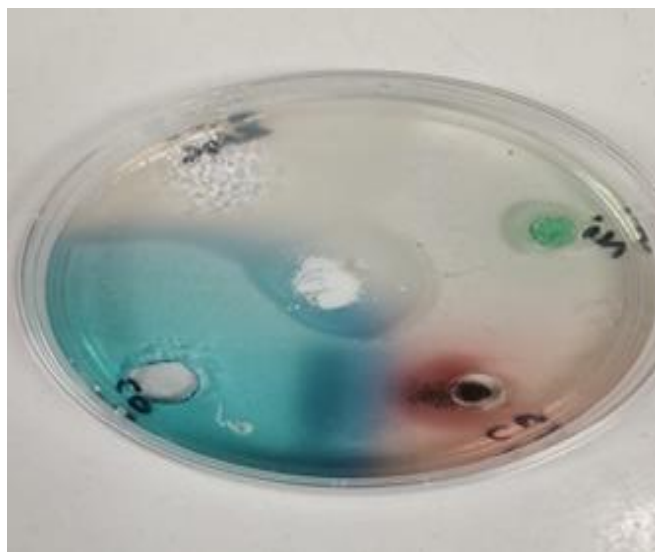


Figure 7: Antibacterial activity of the Zn/Ni(BPyCOOH)₂ bimetallic complex on *Staphylococcus aureus* and *E. coli*, along with control wells

3.7.2. Minimum Inhibitory Concentration:

The minimum inhibitory concentrations (MICs) for the zone of inhibition were determined against four bacterial strains, *i.e.*, Gram-positive (*S. aureus*, and *B. licheniformis*) and Gram-negative bacteria (*E. coli* and

P. mirabilis) at 5, 10, and 20 mg/ml of the Zn/Ni(BPyCOOH)₂ complex. For all bacterial strains, outcomes of Tukey's test revealed that there was a significant variance ($p < 0.05$) in the antibacterial activity at 5, 10 and 20 mg/ml of Zn/Ni(BPyCOOH)₂ complex [34]. The highest zones of inhibition were observed at the highest concentration of Zn/Ni(BPyCOOH)₂ complex (20 mg/ml) with respect to 10 and 5 mg/ml of Zn/Ni(BPyCOOH)₂ complex and positive control erythromycin (5 mg/ml). No zones of inhibition were detected against the negative control (with DMSO solvent only). The diameters of the zone of inhibition of the bacteria are summarized in Figs. 8-9.

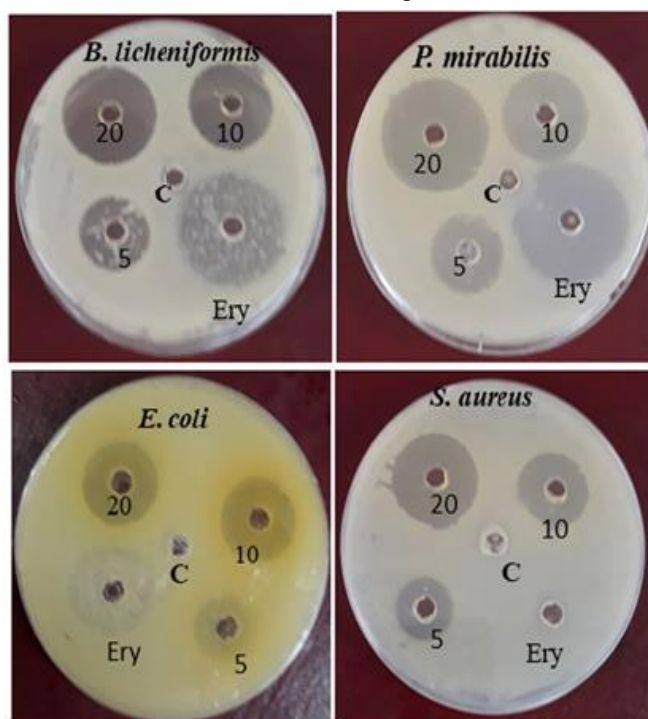


Figure 8: MIC of the zone of inhibition of the Zn/Ni(BPyCOOH)₂ bimetallic complex on *B. licheniformis*, *P. mirabilis*, *Staphylococcus aureus*, and *E. coli*, along with control wells.

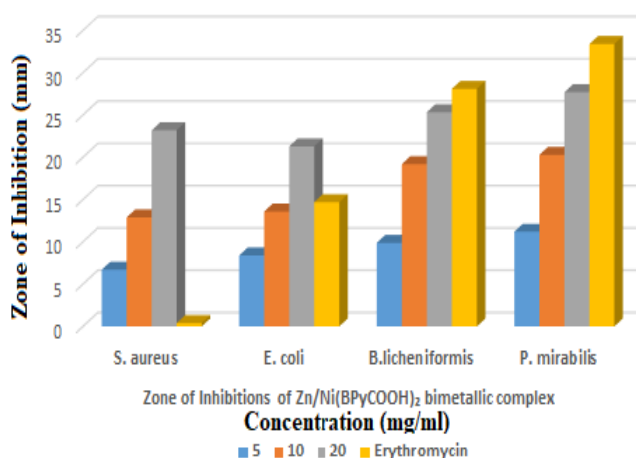


Figure 9: Graph of the zone of inhibition of the Zn/Ni(BPyCOOH)₂ bimetallic complex on *B. licheniformis*, *P. mirabilis*, *Staphylococcus aureus*, and *E. coli*, along with erythromycin (as a positive control).

The results of Table 1 show that Gram-negative bacteria, e.g., *P. mirabilis*, showed the highest zones of inhibition (27.7 ± 0.9) when compared to other bacterial positive strain (*S. aureus*). For *B. licheniformis*, the zone of inhibition (25.33 ± 0.8) was significantly larger than that of *E. coli* (21.3 ± 0.6) at 20 mg/ml concentration of the Zn/Ni(BPyCOOH)₂ complex. No zone of inhibition was found in the positive control group against *S. aureus* at 5 mg/ml of erythromycin, which shows that this bacterial strain is resistant to the antibiotic (erythromycin). *S. aureus* showed zones that were 4 mm bigger than those shown by *E. coli*, and these results showed that the Zn/Ni(BPyCOOH)₂ complex is more reticent to the growth of *S. aureus* than others.

Table 1: The zone of inhibition of the Zn/Ni(BPyCOOH)₂ bimetallic complex on *B. licheniformis*, *P. mirabilis*, *Staphylococcus aureus*, and *E. coli*, along with erythromycin (as a positive control well).

Concentrations	Zone of Inhibitions of Zn/Ni(BPyCOOH) ₂ bimetallic complex			
	<i>S. aureus</i>	<i>E. coli</i>	<i>B. licheniformis</i>	<i>P. mirabilis</i>
5	6.7±0.9	8.4±0.2	9.88±0.3	11.2±0.1
10	12.9±0.3	13.6±0.03	19.2±0.2	20.3±0.7
20	23.2±0.1	21.3 ±0.6	25.33 ±0.8	27.7±0.9
Erythromycin (5mg/ml)	0.4±0.1	14.7±0.2	28.1±0.4	33.4±0.8

4. Conclusion:

In conclusion, a tailored bimetallic Zn/Ni(BPy-COOH)₂ complex was successfully synthesized from substituted 2,2'-bipyridine-4,4'-dicarboxylic acid, demonstrating the effectiveness of rational ligand design in generating multifunctional coordination compounds. UV-Vis and FTIR analyses confirmed the coordination of Zn(II) and Ni(II) ions through nitrogen and oxygen donor sites, resulting in a stable and electronically interactive bimetallic structure. Antimicrobial evaluation revealed that the Zn/Ni(BPy-COOH)₂ complex showed significant activity against *P. mirabilis* at 20 mg/mL and comparable responses to erythromycin at 5 mg/mL. The absence of inhibition in the negative control validated the reliability of the findings.

Conflict of Interests:

The authors declare that they have no conflicts of interest.

Funding:

Not applicable

References

- [1] M.A. Wahba, R.K. Khaled, and M. Dawy, "Tailored bimetallic Zn/Ni and Zn/Ag MCM-41 photocatalysts for enhanced visible-light photocatalytic tetracycline degradation," *Sc. Rep.*, vol. 15, pp. 5725, 2025.
- [2] A.F. Hassan, Kareem, N.H. Al-Haidery S.R. Kareem, S. A. Malik, S. A. Salem Al-Jadaan and N.H. Al-Saadawy, "New charge-transfer complexes of organochalcogenide compound based on aryl acetamide group with quinones: synthesis, characterization, antioxidant, and computational study," *Ind. J. Chem.*, vol. 24, pp. 425-426, 2024.
- [3] T.D.W. Claridge, "High-resolution NMR techniques in organic chemistry," Elsevier: 2016; 27. Edition: 3rd, Publisher: Elsevier, ISBN: 9780080999869, 2018.
- [4] S.K.V. Gohel, S. Palash, G.P. Singh, K. Bhat, and M. Prakash, "Lower melting pharmaceutical cocrystals of metaxalone with carboxamide functionalities," *J. Mol. Struct.*, vol. 1178, pp. 479-490, 2019.
- [5] C. Xu, R. Luo, C. Xie, C. Fan, Y. Fan, and X. Zhang, "Photocatalytic and magnetic properties of two Ni(II) metal-organic complexes based on

- 6,6'-di(benzimidazol-2-yl)-2,2'-bipyridine," *Polyhedron*, vol. 233, pp. 116305, 2023.
- [6] Y. Bo, W. Wu, R. Guo, M. Cao, Y. Liang, M. Wang, W. Yu, L. Zhang, and J. Zhang (2022) Bipyridine Carboxylic Acid as a High-Performance Anode Material for Lithium- and Sodium-Ion Batteries. *Electrochim. Acta*, vol. 405, pp. 139628, 2022.
- [7] S. Yadev, S. P. Sonkar, K. S. Tiwari, and M. Shukla, "A review on sustainable synthesis methods, characterization and applications of inorganic metal complexes: Recent advances and future approaches," *Results Chem.*, vol. 10, pp.101743, 2024.
- [8] N. J. Hales, and J. F. Beattie, "Novel inhibitors of prolyl 4-hydroxylase. 5. The intriguing structure-activity relationships seen with 2, 2'-bipyridine and its 5, 5'-dicarboxylic acid derivatives," *J. Med. Chem.*, vol. 36, pp. 3853-3858, 1993.
- [9] H. L. Huang, Y. J. Liu, C. H. Zeng, J. H. Yao, Z. H. Liang, Z. Z. Li, and F. H. Wu, "Studies of ruthenium(II) polypyridyl complexes on cytotoxicity in vitro, apoptosis, DNA-binding and antioxidant activity," *J. Mol. Struct.*, vol. 966, pp. 136-143, 2010.
- [10] [1T. S. Kamatchi, N. Chitrapriya, V.S.J. Ahmed, S. S. Moon, F.R. Fronczek, and K. Natarajan, "Ruthenium(II) complexes of 2,2'-bipyridine-5,5'-dicarboxylic acid: Synthesis, structure, DNA binding, cytotoxicity and antioxidant activity," *Inorg. Chim. Acta*, vol. 404, pp. 58–67, 2013.
- [11] H. Liu, X. Peng, and H. Zeng, "Synthesis, structure and luminescence property of Eu (III) metal–organic framework based on 2, 2'-bipyridine-5, 5'-dicarboxylic acid," *Inorg. Chem. Commun.*, vol. 46, pp. 39-42, 2014.
- [12] S.H. Tan, H. Luo, D.W. Sun, Z.H. Chen, and G. Q. Zhong, "Two transition metal complexes based on bipyridine dicarboxylate and 1,10-phenanthroline: synthesis, crystal structure, luminescent properties, *SSRN Electronic Journal*, 4019292, pp. 1-20, 2022.
- [13] Y.J. Liu, Z.H. Liang, Z-Z. Li, J. H. Yao, and H-L. Huang, "Cellular uptake, cytotoxicity, apoptosis, antioxidant activity and DNA binding of polypyridyl ruthenium(II) complexes", *J. Organomet. Chem.*, vol. 696, pp. 2728-2735, 2011.
- [14] V. Komreddy, K. Ensz, H. Nguyen, and D. P. Rillema, "Synthesis and characterization of rhenium (I) 4,4'-dicarboxy-2,2'-bipyridine tricarbonyl complexes for solar energy conversion," *Inorg. Chim. Acta*, vol. 511, pp. 119815, 2020.
- [15] H.K. Tanui, (2019) Bimetallic complexes; A mini review of their synthesis, and potential antitumor activities, A Review. DOI: 10.13140/RG.2.2.19269.50400
- [16] M.B. Pastor, (2018). *Bimetallic complexes: The fundamental aspects of metal-metal interactions, ligand sterics and application*. University of the Pacific, Dissertation. https://scholarlycommons.pacific.edu/uop_etds/3559
- [17] S.Y. Al-Qaradawi, A. Mostafa, A.A. Bengali, (2016) "Charge-transfer complexes formed in the reaction of 2-amino-4-ethylpyridine with π -electron acceptors," *J. Mol. Struct.*, vol. 1106, pp. 10–18, 2016.
- [18] R. Zhao, L. Mei, K.Q. Hu, M. Tian, Z.F. Chai, W. Q. Shi, "Bimetallic uranyl organic frameworks supported by transition-metal-ion-based metalloligand Motifs: synthesis, structured, and luminescence properties," *Inorg. Chem.* vol. 57, pp. 6084-6094, 2018.
- [19] Z. Min, M.A.S. Wilmot, C.L. Cahil, M. Andrews, and R. Taylor, "Isorecticular lanthanide metal-organic frameworks: syntheses, structures and photoluminescence of a family of 3D Phenylcarboxylates," *Eur. J. Inorg. Chem.*, vol. 2012, pp. 4419-4426, 2012.
- [20] A.M.P. Santos, A. C. Bertoli, A. C. C. P. Borges, R. A. P. Gomes, J. S. Garcia, and M. G. Trevisan, "New organomineral complex from humic substances extracted from poultry wastes: synthesis, characterization and controlled release study," *J. Braz. Chem. Soc.*, vol. 29, pp. 140-150, 2018.
- [21] P. Li, and J. Hur, "Utilization of UV-VIS spectroscopy and related data analyses for dissolved organic matter (DOM) studies: A review," *Crit. Rev. Env. Sci. Technol.*, vol. 47 pp. 131-154, 2017.
- [22] S. Navalon, A. Dhakshinamoorthy, M. Alvaro, B. Ferrer, and H. Garcia, Metal–organic frameworks as photo-catalysts for solar-driven overall water

- splitting. *Chem. Rev.*, vol. 123, pp. 445–490, 2022.
- [23] N.A. Hadi, F.K. K. AL-Fatlawi, H.A. Khursheed, A. H. Jawad, “Molecular docking, biological evaluation of a Co (II) complex derivative of N⁵, N⁵-di(piperidine-2-carbonyl)-[2,2'-bipyridine]-5,5'-dicarboxamide Ligand,” *Open Access Res. J. Biol. Pharm.*, vol. 14, pp. 053-061, 2025.
- [24] D.A. Skoog, F.J. Holler, and S.R. Crouch, “Principles of Instrumental analysis,” 6th Edition, Brooks Cole, Belmont, pp.1039, 2007.
- [25] B. Yotnoi, M. Sinchow, A. Ngamjarrojana, and A. Rujiwatra, “Crystal structures and photoluminescent properties of highly disordering lanthanide-2, 5-pyridinedicarboxylate frameworks. *Inorg. Chim. Acta*, vol. 500, pp. 119236, 2020.
- [26] B. Yiyang, W. Wanbao, G. Ruitian, and Z. Jiaheng, “Bipyridine carboxylic acid as a high-performance anode material for lithium- and sodium-ion batteries,” *Electrochim. Acta*, vol. 405, pp. 139628, 2022.
- [27] Y. Shailendra, P. S. Sankatha, S. T. Kanha, and S. Mrityunjay, “A review on sustainable synthesis methods, characterization and applications of inorganic metal complexes: Recent advances and future approaches,” *Results Chem.*, vol. 10, pp. 101743, 2024.
- [28] H.A. Khursheed, F.K.K. AL-Fatlawi, and H.S. Buktash, “Synthesis of ferrous complexes 2,2-bipyridine-5,5-dicarboxylic acid and studied for its antioxidant properties,” *Iraqi J. Natur. Sci. Nanotechnol.*, vol. 6, pp. 134-144, 2025.
- [29] C. Tan, S. Hu, J. Liu, and L. Ji, “Synthesis, characterization, antiproliferative and antimetastatic properties of two ruthenium-DMSO complexes containing 2,2'-biimidazole,” *Eur. J. Med. Chem.* vol. 46, pp. 1555-1563, 2011.
- [30] S. Nasiri, M. Rabiei, A. Paleicius, G. Janusus, A. Vilkauskas, V. Nutalapati, and A. Monshi, “Modified Scherrer equation to calculate crystal size by XRD with high accuracy, examples Fe₂O₃, TiO₂ and V₂O₅. *Nano Trends*. vol. 3, pp. 100015, 2023.
- [31] L. Xiang and H. Jean-René, Recent developments in penta-, hexa- and heptadentate Schiff base ligands and their metal complexes, *Coordination Chemistry Reviews*, 389, pp. 94–118, 2019.
- [32] H. Zahid, M. Arif, A. Muhammad and T. Supuran, Metal-based antibacterial and antifungal agents: synthesis, characterization, and in vitro biological evaluation of Co(II), Cu(II), Ni(II), and Zn(II) complexes with amino acid-derived compounds, *Bioinorganic Chemistry and Applications*. (2006) 13, pp. 083131, 2006, https://doi.org/10.1155/BCA/2006/83131_2-s2.0-33846659741.
- [33] A.K. Fayaz, S. Ambreen and Y.T. Mohammad, Synthesis, characterization of Cu(II)/ Ni(II) complexes metal ions derived from flexible dicarboxylate ligand with 2,2'-bipyridine and their photodegradations applications, *Sindh University Research Journal (Science Series) SURJ*, vol. 57, pp. 22-28, 2025, <https://doi.org/10.26692/surjss.57i02.7297>
- [34] M. Kuate, M.A. Conde, K.N. Nchimi, A.G. Paboudam, S.E. Ntum, and P.T. Ndifon, Synthesis, characterization and antimicrobial studies of Co(II), Ni(II), Cu(II) and Zn(II) complexes of (E)-2-(4-dimethylbenzylidimino)-glycylglycine, (glygly-DAB) a schiff base derived from 4-dimethylaminobenzaldehyde and glycylglycine, *International Journal of Organic Chemistry*. vol. 8, pp. 298–308, <https://doi.org/10.4236/ijoc.2018.83022>.